Study of Modal Solution Procedures for Microstrip Step Discontinuities

QIANG XU, KEVIN J. WEBB, MEMBER, IEEE, AND RAJ MITTRA, FELLOW, IEEE

Abstract—**Single and cascaded microstrip step discontinuity problems are studied. Modal formulations and numerical solution procedures are investigated in an effort to determine computationally efficient techniques for the solution of such problems. The enforcement of a modal orthogonality criterion, the boundary enlargement/reduction concept, and convergence as a function of the number of modes and their accuracy are considered. Theoretical and experimental results are presented for the scattering parameters of several example geometries.**

I. INTRODUCTION

MICROSTRIP lines have been used in the microwave frequency range for some time. Recently, microstrip has been used in the millimeter-wave range for purposes of realizing interconnects and a variety of passive components. At these higher operating frequencies accurate component modeling becomes more critical. Many passive components utilize step transitions in the strip width, or step discontinuities. An accurate analysis of these step discontinuities is therefore of the utmost importance in facilitating the design of such components.

At the lower frequencies one may use quasi-static techniques to obtain results for the capacitance associated with a discontinuity [1]. A number of papers have appeared which use Poisson's equation in a spectral-domain formulation [2]. A numerical procedure such as the method of moments (MoM) may then be used to approximately solve for the charge on the strip and the effective "excess" capacitance associated with some discontinuity. Step discontinuities, gaps, and truncated lines have been treated this way. The accuracy of such an analysis obviously deteriorates with increasing frequency. Hence, a full-wave solution technique is necessary if one is to obtain satisfactory results for higher microwave and millimeter-wave frequencies. The full-wave analysis of the two-dimensional microstrip structure is now fairly well developed [3]–[6]. A spectral-domain formulation with a MoM solution yields satisfactory results for the propagating and a few higher order modes, but it is generally impractical to obtain a large number of evanescent modes. Relatively few papers have appeared detailing numerical solution techniques or providing experimental data for three-dimensional microstrip problems. The truncated line problem has been treated using a two-dimensional spectral relationship in the plane of the metallization [7]. Lately the spectral-domain analysis was applied to study the scattering from *E*-plane circuit elements [8]. A judicious choice of the strip expansion functions is necessary to yield good results. An equivalent parallel-plate waveguide model has been used to permit easy evaluation of propagating and evanescent modes [9]–[11], which have then been used in a mode-matching procedure to determine the scattering parameters of some step discontinuity problems. The accuracy of this technique is limited by the accuracy of the parallel-plate waveguide model, which may be a limitation in predicting the phase of the scattering parameters. An alternative is to find approximate full-wave solutions for a number of propagating and evanescent modes and then apply a mode-matching technique. Some data obtained by this approach have appeared [12]. The formulation and convergence mechanisms using this latter and related techniques need to be studied in order to achieve reliable solutions with minimal numerical computation. The mode-matching method has also been applied to the discontinuity problem in various finline structures [13], [14].

New modal formulation techniques are described in this presentation. The eigenmodes are found using a spectral-domain formulation with a MoM solution. The step discontinuity problem is then analyzed using (i) mode matching where mode orthogonality is enforced and (ii) mode matching where mode orthogonality is not assumed and the modes are treated as nonorthogonal basis functions. The motivation for the second approach is that it is difficult to find a large number of eigenmodes and frequently the solutions found may be poor and may not satisfy the mode orthogonality criterion well. A comparison is made between these approaches and experimental results obtained, on the one hand, and data presented in the literature, on the other. The modal formulation techniques are developed, with a discussion of the relative merits of the procedures adopted. Numerical and experimental results are provided for single and double step discontinuity problems.

II. MODAL ANALYSIS FORMULATION

The two-dimensional microstrip geometry is shown in Fig. 1. A finite set of eigenvalues (phase constants) and eigenfunctions (mode functions) need to be determined for

Manuscript received April 15, 1987; revised April 18, 1988. This work was supported by Martin Marietta Laboratories and by the University of Maryland Minta Martin Aeronautical Fund and General Research Board.

Q. Xu and K. J. Webb are with the Electrical Engineering Department, University of Maryland, College Park, MD 20742.

R. Mittra is with the Department of Electrical and Computer Engineering, University of Illinois, Urbana, IL 61801.

IEEE Log Number 8824993.

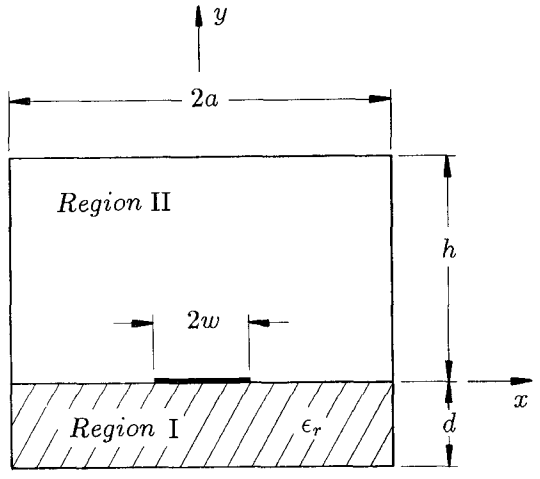

Fig. 1. Shielded microstrip cross section.

inclusion in the discontinuity representation. Perfect electric conductors (pec's) and isotropic dielectrics are assumed in each region.

A spectral Green's function relationship relating the currents and fields in the plane of the strip can be expressed as [4]

$$\begin{pmatrix} \tilde{Z}_{xx}(\alpha_n,\beta) & \tilde{Z}_{xz}(\alpha_n,\beta) \\ \tilde{Z}_{zx}(\alpha_n,\beta) & \tilde{Z}_{zz}(\alpha_n,\beta) \end{pmatrix} \begin{pmatrix} \tilde{J}_x(\alpha_n) \\ \tilde{J}_z(\alpha_n) \end{pmatrix} = \begin{pmatrix} \tilde{E}_{x0}(\alpha_n) \\ \tilde{E}_{z0}(\alpha_n) \end{pmatrix}. \quad (1)$$

The equivalent transmission line method used to derive the Green's function can be easily extended for more complicated structures such as multiple dielectric layers or multiple strip planes. The MoM, specifically Galerkin's method, is applied to solve for the eigenvalues and eigenfunctions. The strip currents are represented approximately by a finite set of appropriate basis functions with unknown coefficients. The basis functions used are [15]

$$f_{xi}(x) = \frac{\cos[(i-1)\pi(x/w+1)]}{\sqrt{1-(x/w)^2}} \quad (2a)$$

$$f_{zj}(x) = \frac{\sin[j\pi(x/w+1)]}{\sqrt{1-(x/w)^2}} \quad (2b)$$

where $i=1,2,\cdots,I$ and $j=1,2,\cdots,J$ with $-w \leqslant x \leqslant w$. Upon performing inner products, a matrix equation is obtained which can be solved iteratively using Newton's method to determine the eigenvalues. The relative basis function coefficients can then be computed. This is quite a time-consuming process if a large number of higher order modes are needed for a mode-matching formulation. The mode functions can be found either by returning to the transverse transmission line model or by evaluating the scalar potential coefficients using the appropriate boundary conditions on the fields.

Waveguide step discontinuities are of two types: boundary reduction and boundary enlargement, using the terminology of Wexler [16]. A boundary reduction occurs when the waveguide cross section for the incident wave is larger than that for the transmitted wave, the reverse being

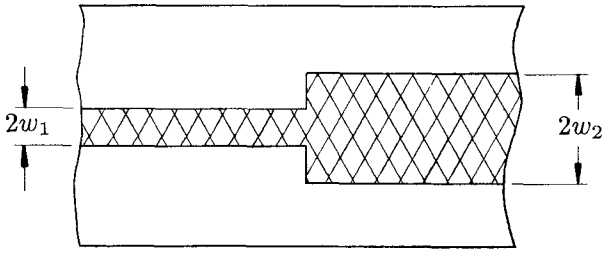

Fig. 2. Single step discontinuity in strip width.

boundary enlargement. The difference in the formulation for the two problems is in the definition of the inner product, which optimizes the convergence of the solution as a function of the number of modes used. For many waveguide discontinuities, such as those in circular or rectangular waveguide, boundary enlargement and boundary reduction are well defined. This is not the case for microstrip, as the waveguide shield has the same dimension on both sides of the strip discontinuity. Therefore, the definition of boundary enlargement or reduction must be carefully studied to obtain optimally convergent solutions with a relatively small number of modes.

Consider the microstrip step discontinuity shown in Fig. 2. By matching the transverse fields in the plane of the discontinuity, one obtains

$$\sum_{p=1}^{P} \left[a_p^{(1)} + b_p^{(1)}\right] \boldsymbol{e}_p^{(1)} = \sum_{q=1}^{Q} \left[a_q^{(2)} + b_q^{(2)}\right] \boldsymbol{e}_q^{(2)} \quad (3a)$$

$$\sum_{p=1}^{P} \left[a_p^{(1)} - b_p^{(1)}\right] \boldsymbol{h}_p^{(1)} = \sum_{q=1}^{Q} \left[-a_q^{(2)} + b_q^{(2)}\right] \boldsymbol{h}_q^{(2)} \quad (3b)$$

where $\boldsymbol{e}(x, y)$ and $\boldsymbol{h}(x, y)$ are normalized transverse vector electric and magnetic mode functions, respectively, and the a's are the incident and the b's the reflected mode coefficients. The superscripts refer to region 1 for $z<0$ and region 2 for $z>0$. In order to solve (3), an inner product is introduced which is defined as

$$\langle \boldsymbol{e}_i^{(\nu)}(x,y), \boldsymbol{h}_j^{(\lambda)}(x,y)\rangle = \int_S \boldsymbol{e}_i^{(\nu)}(x,y) \times \boldsymbol{h}_j^{(\lambda)}(x,y) \cdot d\boldsymbol{s} \quad (4)$$

where $\nu=1$ or 2 and $\lambda=1$ or 2, indicating the quantities for $z<0$ and $z>0$, respectively, and S is the shield cross section. When boundary enlargement or reduction is clearly defined, the most rapid convergence is obtained when the inner product is defined such that the electric field is taken from the smaller waveguide and the magnetic field from the larger waveguide because of the effective enforcement of the junction boundary conditions through the inner products [16], [17]. This enables the boundary conditions at the junction to be satisfied fairly well with a minimum number of modes. Upon performing inner products on (3), the resulting set of equations can be written as

$$(M_{11})((A^{(1)}) + (B^{(1)})) = (M_{12})((A^{(2)}) + (B^{(2)})) \quad (5a)$$

$$(M_{21})((A^{(1)}) - (B^{(1)})) = (M_{22})(-(A^{(2)}) + (B^{(2)})) \quad (5b)$$

where

$$(M_{11}) = (M_{11}^r) = (M_{21}^e)$$
$$(M_{12}) = (M_{12}^r) = (M_{11}^e)$$
$$(M_{21}) = (M_{21}^r) = (M_{22}^e)$$
$$(M_{22}) = (M_{22}^r) = (M_{12}^e).$$

The superscripts refer to the boundary reduction (r) and enlargement (e) formulations, respectively, and the A and B matrices contain the mode coefficients for the incident and the reflected field, respectively.

For the microstrip formulation presented here, the inner product is performed in the spectral domain to keep the computation consistent with the mode solutions of the uniform microstrip. The inner product in the spectral domain is

$$\langle \tilde{\boldsymbol{e}}_i^{(\nu)}, \tilde{\boldsymbol{h}}_j^{(\lambda)} \rangle = \frac{1}{4a} \sum_{n=-\infty}^{+\infty} \int_0^{d+h} \left[\tilde{e}_{ix}^{(\nu)}(\alpha_n, y) \tilde{h}_{jy}^{(\lambda)}(-\alpha_n, y) - \tilde{e}_{iy}^{(\nu)}(\alpha_n, y) \tilde{h}_{jx}^{(\lambda)}(-\alpha_n, y) \right] dy. \quad (6)$$

In (6) the y integral can be carried out analytically.

The eigenmodes of a waveguide with perfectly conducting walls satisfy the standard orthogonality relationship [18]:

$$\int_S \boldsymbol{e}_i \times \boldsymbol{h}_j \cdot d\boldsymbol{s} = \delta_{ij} \quad (7)$$

where δ_{ij} is the Kronecker delta. In the case of waveguides with perfectly conducting walls and lossless isotropic dielectric media, an alternative orthogonality condition can be used:

$$\int_S \boldsymbol{e}_i \times \boldsymbol{h}_j^* \cdot d\boldsymbol{s} = \delta_{ij}. \quad (8)$$

As a result of the orthogonality relationship, (M_{11}) and (M_{22}) in (5) reduce to diagonal matrices. Thus (M_{11}) and (M_{22}) need not be evaluated if the eigenmodes are normalized. As the microstrip mode solutions are approximate, the orthogonality condition serves as a test of the accuracy of these numerically computed modes. Meanwhile, it introduces the question of whether or not to retain those matrix elements which theoretically should equal zero.

The solutions of (5) can be represented in the form of a generalized scattering matrix which includes information on the dominant as well as the higher order modes and is expressed as

$$\begin{pmatrix} (B^{(1)}) \\ (B^{(2)}) \end{pmatrix} = \begin{pmatrix} (S_{11}) & (S_{12}) \\ (S_{21}) & (S_{22}) \end{pmatrix} \begin{pmatrix} (A^{(1)}) \\ (A^{(2)}) \end{pmatrix}. \quad (9)$$

A more detailed discussion of the generalized scattering matrix can be found in [8], [11], and [19].

The double step problem of Fig. 3 can be analyzed using an extension of this technique, where the generalized scattering parameters for each of the two step discontinuities can be combined with the transmission matrix of the intervening length of line (effectively cascading three transmission matrices). With some manipulations, a composite generalized scattering matrix for the double step can be obtained [11].

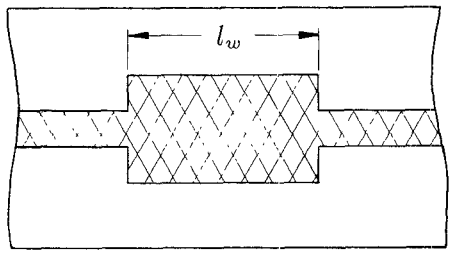

Fig. 3. Double step discontinuity.

III. Numerical and Experimental Results

Results are presented for single and double step discontinuities in shielded microstrip where the shield is sufficiently large so as to have negligible effect on the strip currents. Satisfactory results for the double step rely on good results for the single step.

To ensure the accuracy and the stability of the modal analysis results, several parameters can be determined during the computation. First, the conservation of power for a single propagating mode can be expressed as $|S_{11}|^2 + |S_{21}|^2 = 1$, which is not a sufficient condition to guarantee a correct solution, but it is necessary and should be verified. Second, it is important to know the effect on the solution of perturbations in the matrix elements, since these elements are approximate. A measure of this can be obtained from the condition number of the operator matrix A in the equation $Ax = b$, where x represents the mode coefficient matrix. The condition number is defined here as

$$C(A) = \left(\frac{\lambda_{\max}}{\lambda_{\min}} \right)^{1/2} \quad (10)$$

where $\lambda_{\max}$ and $\lambda_{\min}$ are the maximum and minimum eigenvalues of the matrix $A^H A$. A^H is defined as the Hermitian, or transposed complex conjugate of A. The matrix A is well conditioned if the condition number $C(A)$ is close to one and ill conditioned when it is significantly greater than one. As a consequence of an ill-conditioned matrix, small errors in the matrix elements could generate large errors in the solution. When the mode functions are not normalized, $C(A)$ can be quite large, resulting in unstable solutions. If A is "preconditioned" by normalizing all the mode functions such that (7) or (8) for $i = j$ results in a number with magnitude one, a dramatic improvement in $C(A)$ results. A typical value of the condition number for normalized mode functions found in this work is about 2.5, which is acceptable.

As the mode functions and the inner products are computed numerically, some deviation from the exact orthogonality relationship is expected. Therefore, in the computed matrix A the value of the nondiagonal elements in (M_{11}) and (M_{22}) reflects the accuracy of the numerical mode solutions. The inner products between different eigenmodes from either the left side or the right side of the junction, with ten modes in each region, result in normal-

TABLE I
SCATTERING PARAMETER COMPUTED ASSUMING ORTHOGONALITY RELATIONSHIP

Assuming Orthogonolity Relationship $< e, h >$		
Frequency	$\lvert S_{11} \rvert$	ϕ_{11}
2.0 (GHz)	0.395	178.7°
10.0 (GHz)	0.661	172.8°

$I=1$, $P=Q=6$, $N=100$, $\epsilon_r=2.32$, $a=17.233$ mm, $h=15.8$ mm, $d=1.58$ mm, $w_1=2.25$ mm, $w_2=7.825$ mm.

TABLE II
SCATTERING PARAMETER COMPUTED BY AN ALTERNATE DEFINITION OF INNER PRODUCT

Assuming Orthogonality Relationship $< e, h^* >$		
Frequency	$\lvert S_{11} \rvert$	ϕ_{11}
2.0 (GHz)	0.3944	178.42
10.0 (GHz)	0.653	177.36

Same parameters as in Table I.

TABLE III
SCATTERING PARAMETER COMPUTED WITHOUT ASSUMING ORTHOGONALITY RELATIONSHIP

Not Assuming Orthogonality Relationship $< e, h >$		
Frequency	$\lvert S_{11} \rvert$	ϕ_{11}
2.0 (GHz)	0.3946	178.66°
10.0 (GHz)	0.667	175.30°

Same parameters as in Table I.

ized inner products less than 0.1 for one basis function ($I=J=1$) and less than 0.01 for three basis functions ($I=J=3$), assuming that the modes are normalized according to (7). Satisfactory results were obtained for the geometries used in this work using inner products with 200 spectral terms (single-sided summation) when one basis function was used, while for three basis functions 400 terms were necessary, the larger number for the latter case being expected because of the more rapid current/field variation. There is a 2 Mbyte memory requirement for computing the scattering matrix for $P=Q=6$ and it takes about 5 minutes on a VAX 11/785 once the mode solutions have been found. Finding the higher order modes can be difficult and requires considerable interactive time.

The significance of the different testing procedures on (3) is now reviewed with a single mode incident from region 1 in Fig. 2. The inner products can be taken according to (7) or (8). A comparison of the two approaches can be seen by comparing Table I, using (7), with Table II, using (8), for $P=Q=6$. For propagating modes, both (7) and (8) give the same result. For illustrative purposes, the remainder of the work presented here uses the inner product definition in (7). The computed reflection coefficient evaluated without the modal orthogonality assumption, (7), is given in Table III. As the mode solutions in this case were quite good, the results using the two approaches are close. For less accurate mode solutions, the results differ by a greater degree, as would be expected. For poor mode solutions it appears that the conservation of power relationship is satisfied more closely when orthogonality is assumed. Therefore, the orthogonality relation is enforced for better convergence.

TABLE IV
COMPARISON OF BOUNDARY REDUCTION AND ENLARGEMENT TESTING PROCEDURES WITH $P=Q=6$

Comparison of Testing Procedures		
	$\lvert S_{11} \rvert$	$\lvert S_{21} \rvert$
Reduction	0.1729	0.9849
Enlargement	0.4667	0.8844

$\epsilon_r=2.2$, $a=1.6$ mm, $h=1.27$ mm, $d=0.127$ mm, $w_1=0.1905$ mm, $w_2=0.381$ mm, $f=4.0$ GHz.

The boundary enlargement/reduction concept is now addressed. Table IV gives data comparing the boundary enlargement and boundary reduction formulations for a particular single step discontinuity. Six modes from either side of the discontinuity were used in the construction of Table IV with a single mode incident from region 1 in Fig. 2. The parameters correspond to the geometry for which experimental data were obtained. The number of modes was not large enough to obtain reasonable convergence, resulting in some difference between the two approaches. The measured result of $|S_{11}|=0.243$ at 4 GHz indicates that for $P=Q=6$ the boundary reduction formulation provides a result below the measured value and the boundary enlargement formulation a solution above the measured result. There is in general some oscillation of the scattering parameters as a function of the number of modes used. The difference between the two formulations diminishes as the number of modes increases. For the cases studied, the boundary reduction formulation gave the fastest convergence. One could consider that, in the plane of the strip, a step from small to larger strip width corresponds to a one-dimensional boundary reduction, as the support of the electric field tangential to the strip has been reduced. For the remainder of the results presented here, the boundary reduction formulation is used in (5).

If the modes used are accurate enough, the differences in the orthogonality criterion and, if there is a sufficient number, the boundary enlargement–boundary reduction formulations should be negligible. The purpose of this comparison was to determine procedures to obtain the most rapid convergence as a function of both the number of modes and their accuracy.

In a modal analysis, the convergence as a function of the total number of modes and as a function of the ratio of the number of modes used on either side of the junction P/Q, or relative convergence, needs to be addressed. The criterion used in this convergence study consists of the values of the scattering parameters. As an example, Fig. 4 gives calculated data for $|S_{11}|$ as a function of $P+Q$ for a particular geometry given in [10]. For each curve, the number of modes taken from the right-hand side of the junction is fixed while the number of modes from the left

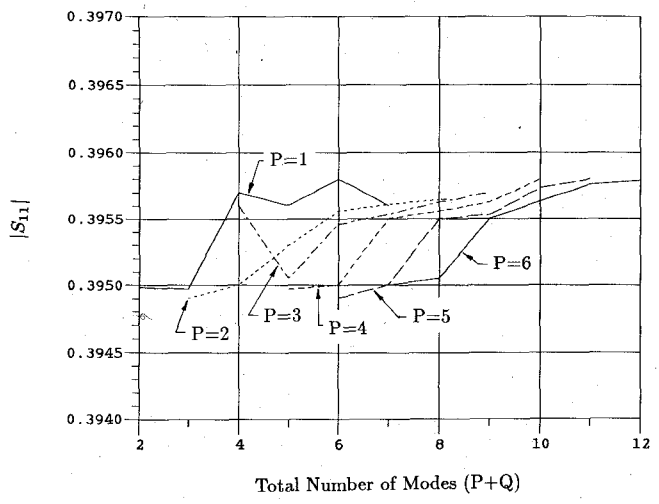

Fig. 4. Relative convergence of the magnitude of the reflection coefficient as a function of the number of modes used ($\epsilon_r = 2.32$, $a = 17.233$ mm, $h = 15.8$ mm, $d = 1.58$ mm, $w_1 = 2.25$mm, $w_2 = 7.825$ mm, $f = 2.0$ GHz).

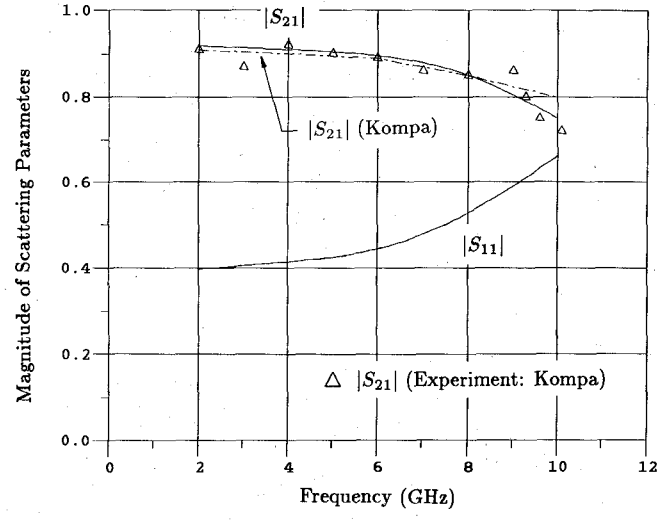

Fig. 5. Magnitude of the scattering parameters as a function of frequency ($\epsilon_r = 2.23$, $a = 17.233$ mm, $h = 15.8$ mm, $d = 1.58$ mm, $w_1 = 2.25$ mm, $w_2 = 7.825$ mm). The solid curve represents the computed results of this work, the dashed represents that of the equivalent waveguide model used by Kompa.

side is varied as indicated. For this particular case $|S_{11}|$ was not very sensitive to the number of modes used. No significant effect of the ratio P/Q has been observed. A considerably larger number of modes may be required to guarantee a convergent solution for a particular geometry, especially for the phase. These numerical data do not support the use of a mode ratio different from $P = Q$. An equal number of modes on either side of the junction were therefore used.

Computed magnitudes of S_{11} and S_{21} are plotted as a function of frequency in Fig. 5 for a geometry used by Kompa [9]. At higher frequencies (around 10 GHz), some difference between the theoretical and experimental data in [9] is observed, which is probably due to the accuracy of the equivalent waveguide model used and a second propagating mode with a cutoff frequency of about 9.8 GHz. The theory presented here is in close agreement with these experimental results. The equivalent waveguide model appears to predict the magnitude of the scattering parameters fairly well under appropriate conditions, but the phase accuracy is not evident.

TABLE V
CONVERGENCE IN THE SCATTERING PARAMETERS FOR A SINGLE STEP DISCONTINUITY AS A FUNCTION OF THE NUMBER OF CURRENT BASIS FUNCTIONS AND MODES

Convergence in the Scattering Parameters			
Modes	Basis Functions	S_{11}	S_{21}
6	1	$(-0.1299, 0.3756)$	$(0.81708, 0.2892)$
6	3	$(-0.1729, 1.346 \times 10^{-4})$	$(0.9849, -8.359 \times 10^{-5})$
10	1	$(-0.2370, -0.6132)$	$(0.5877, 0.4717)$
10	3	$(-0.2706, -1.73 \times 10^{-4})$	$(0.9627, -2.08 \times 10^{-4})$

$\epsilon_r = 2.2$, $a = 1.6$ mm, $h = 1.27$ mm, $d = 0.127$ mm, $w_1 = 0.1905$ mm, $w_2 = 0.381$ mm, $f = 4$ GHz.

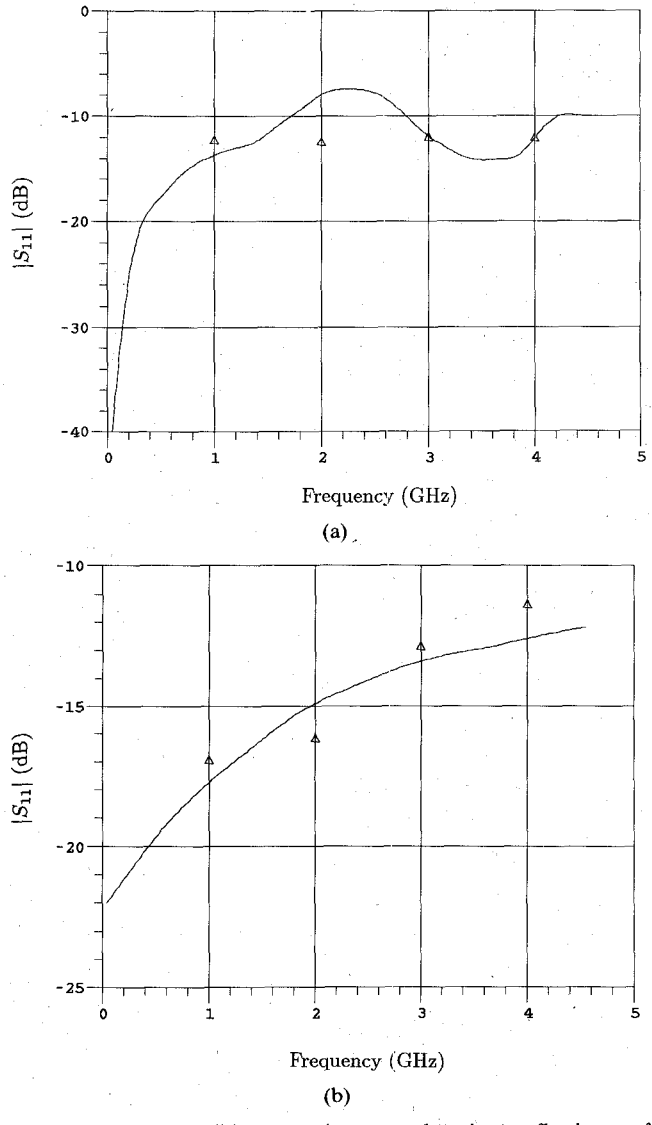

Fig. 6. Measured (solid line) and computed (points) reflection coefficient for (a) a single step-discontinuity ($\epsilon_r = 2.2$, $a = 1.6$ mm, $h = 1.27$ mm, $d = 0.127$ mm, $w_1 = 0.1905$ mm, $w_2 = 0.381$ mm) and (b) a double step-discontinuity (geometry same as (a) with $l_w = 5.08$ mm).

Experiments have been performed on single and double step discontinuities with different step ratios. For a single step discontinuity with a line width ratio of $w_2/w_1 = 2$, the convergence in the scattering parameters as a function of the number of modes and the number of current expansion functions is given in Table V. For this problem ten modes either side of the junction and three basis functions for the strip currents give satisfactory results. Notice that a larger number of modes with a poor representation for the strip currents do not provide an improvement in the results. For reasonable convergence in both magnitude and phase, more than six modes are necessary. Single and double step discontinuity experimental results for $|S_{11}|$ are given in Fig. 6, together with computed results using $P = Q = 10$. The agreement between theory and experiment is quite good. Possible sources for any discrepancy are the number of modes used and the effects of finite conductor thickness and loss, which are not included in the current theory.

IV. Conclusion

New aspects of the modal analysis technique, as applied to the microstrip discontinuity problem, have been investigated. Items discussed were the merits of enforcing modal orthogonality, the inner product definition, the boundary enlargement/reduction concept, and convergence. The purpose of this study was to find satisfactory numerical solutions with minimum computational requirements. Best results were obtained by enforcing mode orthogonality, and the scattering parameters were generally fairly insensitive to which of the two orthogonality conditions were used, the ratio of the number of modes used on either side of the junction, and whether a boundary enlargement or boundary reduction formulation was used, provided a sufficient number of accurate modes were used.

References

[1] P. Benedek and P. Silvester, "Equivalent capacitances for microstrip gaps and steps," *IEEE Trans. Microwave Theory Tech.*, vol. MTT-20, pp. 729–733, Nov. 1972.

[2] Y. Rahmat-Samii, T. Itoh, and R. Mittra, "A spectral domain analysis for solving microstrip discontinuity problems," *IEEE Trans. Microwave Theory Tech.*, vol. MTT-22, pp. 372–378, Apr. 1974.

[3] T. Itoh and R. Mittra, "Spectral domain approach for calculating the dispersion characteristic of microstrip lines," *IEEE Trans. Microwave Theory Tech.*, vol. MTT-21, pp. 496–499, July 1973.

[4] T. Itoh, "Spectral domain immittance approach for dispersion characteristics of generalized printed transmission lines," *IEEE Trans. Microwave Theory Tech.*, vol. MTT-28, pp. 733–737, July 1980.

[5] R. H. Jansen, "Unified user-oriented computation of shielded, covered, and open planar microwave and millimeter-wave transmission-line characteristics," *Proc. Inst. Elec. Eng.*, pt. H, vol. MOA-1, pp. 14–22, Jan. 1979.

[6] R. H. Jansen, "The spectral-domain approach for microwave integrated circuits," *IEEE Trans. Microwave Theory Tech.*, vol. MTT-33, pp. 1043–1056, Oct. 1985.

[7] P. B. Katehi and N. G. Alexopoulos, "Frequency-dependent characteristics of microstrip discontinuities in millimeter-wave integrated circuits," *IEEE Trans. Microwave Theory Tech.*, vol. MTT-33, pp. 1029–1035, Oct. 1985.

[8] Q. Zhang and T. Itoh, "Spectral-domain analysis of scattering from *E*-plane circuit element," *IEEE Trans. Microwave Theory Tech.*, vol. MTT-35, pp. 138–150, Feb. 1987.

[9] G. Kompa, "*S*-matrix computation of microstrip discontinuities with a planar waveguide model," *Arch. Elek. Übertragung.*, vol. 30, pp. 58–64, Feb. 1975.

[10] N. H. L. Koster and R. H. Jansen, "The microwave step discontinuity: A revised description," *IEEE Trans. Microwave Theory Tech.*, vol. MTT-34, pp. 213–222, Feb. 1986.

[11] T. S. Chu and T. Itoh, "Generalized scattering matrix method for analysis of cascaded and offset microstrip step discontinuities," *IEEE Trans. Microwave Theory Tech.*, vol. MTT-34, pp. 280–284, Feb. 1986.

[12] L.-P. Schmidt, "Rigorous computation of the frequency dependent properties of filters and coupled resonators from transverse microstrip discontinuities," in *Proc. 10th European Microwave Conf.*, 1980, pp. 436–440.

[13] K. Uhde, "Discontinuities in finlines on semiconductor substrate," *IEEE Trans. Microwave Theory Tech.*, vol. MTT-34, pp. 1499–1507, Dec. 1986.

[14] M. Helard, J. Citerne, O. Picon, and V. Fouad Hanna, "Theoretical and experimental Investigation of Finline discontinuities," *IEEE Trans. Microwave Theory Tech.*, vol. MTT-33, pp. 994–1003, Oct. 1985.

[15] L. P. Schmidt and T. Itoh, "Spectral domain analysis of higher-order modes in finline," *IEEE Trans. Microwave Theory Tech.*, vol. MTT-28, pp. 981–985, Sept. 1980.

[16] A. Wexler, "Solution of waveguide discontinuities by modal analysis," *IEEE Trans. Microwave Theory Tech.*, vol. MTT-15, pp. 508–517, Sept. 1967.

[17] L. Carin, K. J. Webb, and S. Weinreb, "Matched windows in circular waveguide," *IEEE Trans. Microwave Theory Tech.*, vol. 36, pp. 1359–1362, Sept. 1988.

[18] R. E. Collin, *Field Theory of Guided Waves*. New York: McGraw Hill, 1960.

[19] H. Patzelt and F. Arndt, "Double-plane steps in rectangular waveguides and their application for transformers, irises, and filters," *IEEE Trans. Microwave Theory Tech.*, vol. MTT-30, pp. 771–776, May 1982.

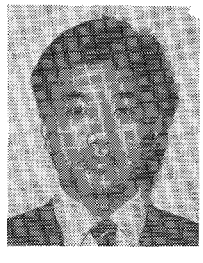

Qiang Xu was born in Beijing, China, in 1959. He received the B.S. degree in physics from Peking University, Beijing, China, in 1982 and the M.S. degree in electrical engineering from the University of Maryland, College Park, in 1987. His current work involves research on microwave and millimeter-wave integrated circuits and the development of finline leaky wave antennas.

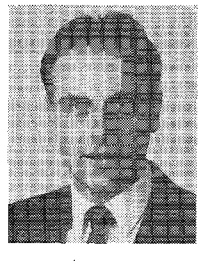

Kevin J. Webb (S'80–M'84) was born in Stawell, Victoria, Australia, on July 7, 1956. He received the B.Eng. and M.Eng. degrees in communication and electronic engineering from the Royal Melbourne Institute of Technology, Australia, in 1978 and 1980, respectively, the M.S.E.E. degree from the University of California, Santa Barbara, in 1981, and the Ph.D. degree in electrical engineering from the University of Illinois, Urbana, in 1984.

Since 1984, he has been an Assistant Professor in the Electrical Engineering Department at the University of Maryland,

College Park. His research interests include numerical electromagnetics, frequency selective surfaces, millimeter-wave and microwave integrated circuits, VLSI circuits, and optoelectronics.

Dr. Webb is a member of Tau Beta Pi, Eta Kappa Nu, and Phi Kappa Phi.

✠

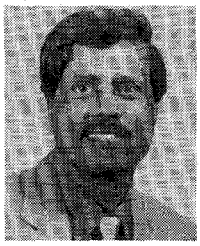

Raj Mittra (S'54–M'57–SM'69–F'71) is the Director of the Electromagnetic Communication Laboratory of the Electrical and Computer Engineering Department and Research Professor of the Coordinated Science Laboratory at the University of Illinois. He is a Past-President of AP-S, and he has served as the editor of the IEEE TRANSACTIONS ON ANTENNAS AND PROPAGATION. He is President of RM Associates, a consulting organization providing services to several industrial and governmental organizations.

Dr. Mittra's professional interests include the areas of analytical and computer-aided electromagnetics, high-speed digital circuits, radar scattering, satellite antennas, microwave and millimeter-wave integrated circuits, frequency selective surfaces, EMP and EMC analysis, and remote sensing.